

Nuclear matter properties with nucleon-nucleon forces up to fifth order in the chiral expansion

Jinniu Hu^{a,1}, Ying Zhang^b, Evgeny Epelbaum^c, Ulf-G. Meißner^{d,e}, Jie Meng^{f,g,h}

^a*School of Physics, Nankai University, Tianjin 300071, China*

^b*Department of Physics, School of Science, Tianjin University, Tianjin 300072, China*

^c*Institut für Theoretische Physik II, Ruhr-Universität Bochum, D-44780 Bochum, Germany*

^d*Institut für Kernphysik, Institute for Advanced Simulation and Jülich Center for Hadron Physics, Forschungszentrum Jülich, D-52425 Jülich, Germany*

^e*Helmholtz-Institut für Strahlen- und Kernphysik and Bethe Center for Theoretical Physics, Universität Bonn, D-53115 Bonn, Germany*

^f*School of Physics and State Key Laboratory of Nuclear Physics and Technology, Peking University, Beijing 100871, China*

^g*School of Physics and Nuclear Energy Engineering, Beihang University, Beijing 100191, China*

^h*Department of Physics, University of Stellenbosch, Stellenbosch 7602, South Africa*

Abstract

The properties of nuclear matter are studied using state-of-the-art nucleon-nucleon forces up to fifth order in chiral effective field theory. The equations of state of symmetric nuclear matter and pure neutron matter are calculated in the framework of the Brueckner-Hartree-Fock theory. We discuss in detail the convergence pattern of the chiral expansion and the regulator dependence of the calculated equations of state and provide an estimation of the truncation uncertainty. For all employed values of the regulator, the fifth-order chiral two-nucleon potential is found to generate nuclear saturation properties similar to the available phenomenological high precision potentials. We also extract the symmetry energy of nuclear matter, which is shown to be quite robust with respect to the chiral order and the value of the regulator.

Keywords: Chiral nucleon-nucleon force, nuclear matter, Brueckner-Hartree-Fock theory

1. Introduction

The nuclear force, a residual strong force between colorless nucleons, lies at the very heart of nuclear physics. Enormous progress has been made towards its quantitative understanding since the seminal work by Yukawa on the one-pion-exchange mechanism, which has been published more than eight decades ago [1]. Already in the fifties of the last century, Taketani *et al.* have pointed out that the range of nucleon-nucleon (NN) potential can be divided into three distinct regions [2]. While the long-distance interaction is dominated by one-pion exchange, the two-pion exchange mechanism plays an important role in the intermediate region of $r \sim 1 \dots 2$ fm. Multi-pion exchange interactions are most essential in the core region. After the discovery of heavy mesons, the NN potential was successfully modeled using the one-boson-exchange (OBE) picture [3, 4] with multi-pion exchange potentials being effectively parametrized by single exchanges of heavy mesons like σ -, ω - and ρ -mesons. With a fairly modest number of adjustable parameters, the OBE potential models such as the Bonn [5, 6] and Nijmegen 93 [7] models were able to achieve a semi-quantitative description of NN scattering data. Furthermore, based on the general operator structure of the two-nucleon interaction in coordinate space, a phenomenological NN potential model was also developed by the Argonne group [8]. In the 1990s, high-precision charge-dependent NN potential models such as e.g. the Reid93 and Nijmegen I, II [7], AV18 [9] and the CD Bonn [10] potentials have been developed, which describe the available proton-proton and neutron-proton elastic scattering data with $\chi^2/\text{datum} \sim 1$.

¹hujinniu@nankai.edu.cn

While phenomenologically successful, the above mentioned high-precision NN potentials have no clear relation to quantum chromodynamics (QCD), the underlying theory of the strong interactions. Further, they do not provide a straightforward way to generate consistent and systematically improvable many-body forces and exchange currents and do not allow to estimate the theoretical uncertainty. In this sense, a more promising and systematic approach to nuclear forces and current operators has been proposed by Weinberg in the framework of chiral effective field theory (EFT) based on the most general effective chiral Lagrangian constructed in harmony with the symmetries of QCD [11, 12, 13]. The first quantitative studies of NN scattering up to next-to-next-to-leading order ($N^2\text{LO}$) in the chiral expansion have been carried out by Ordóñez *et al.* [14, 15] using time-ordered perturbation theory, see also [16, 17] where the calculations were done using the method of unitary transformations. In the early 2000s, the NN potential has been worked out to fourth order in the chiral expansion ($N^3\text{LO}$) by Epelbaum, Glöckle and Meißner [18] and by Entem and Machleidt [19] based on the expressions for the pion exchange contributions derived by Kaiser [20, 21, 22]. The corresponding three- and four-nucleon forces have also been worked out to $N^3\text{LO}$ [23, 24, 25, 26, 27], see [28, 29] for review articles and [30, 31, 32] for calculations beyond $N^3\text{LO}$. Recently, fifth- ($N^4\text{LO}$) and even some of the sixth-order contributions to the two-nucleon force have been worked out in [33, 34], and a new generation of chiral NN potentials up to $N^4\text{LO}$ utilizing a local coordinate-space regulator for the long-range terms has been introduced in [35, 36]. In parallel, a novel simple approach for estimating the theoretical uncertainty from the truncation of the chiral expansion has been proposed in [35] and successfully validated for two-nucleon observables [35, 36]. The algorithm makes use of the explicit knowledge of the contributions to an observable of interest at various orders in the chiral expansion without relying on cutoff variation. The new state-of-the-art NN potentials confirm a good convergence of the chiral expansion for nuclear forces and lead to accurate description of Nijmegen phase shifts [37]. For related recent developments see Refs. [38, 39].

Currently, work is in progress by the recently established Low Energy Nuclear Physics International Collaboration (LENPIC) [40] towards including the consistently regularized three-nucleon force (3NF) at $N^3\text{LO}$ in ab initio calculations of light- and medium-mass nuclei. In parallel, the novel chiral NN potentials have been tested in nucleon-deuteron elastic scattering and properties of ^3H , ^4He , and ^6Li [41] and selected electroweak processes [42], where special focus has been put on estimating the theoretical uncertainty at each order of the expansion. These studies have revealed the important role of the 3NF, whose expected contributions to various bound and scattering state observables appear to be in good agreement with the expectation based on the power counting.

Light- and medium-mass nuclei can nowadays be studied using various ab initio methods such as the Green's function Monte Carlo method [43], the self-consistent Green's function method [44], the coupled-cluster approach [45], nuclear lattice simulations [46, 47, 48] or the no-core-shell model [49], see also Ref. [50] for a first application of the relativistic Brueckner-Hartree-Fock theory to finite nuclei. Infinite nuclear matter has also been widely studied based on various versions of the chiral potentials using e.g. the quantum Monte Carlo approach [38], self-consistent Green's function method [51, 52], the coupled-cluster method [53], many-body perturbation theory [54], functional renormalization group (FRG) method [55, 56] and the Brueckner-Hartree-Fock (BHF) theory [57, 58]. Recently, Sammarruca *et al.* have discussed the convergence of chiral EFT in infinite nuclear matter using the nonlocal NN potentials up to $N^3\text{LO}$ [19] and including the 3NF at the $N^2\text{LO}$ (i.e. Q^3) level [59]. Fairly large deviations between the results at different chiral orders as compared with the spread in predictions due to the employed cutoff variation have been reported in that paper. This suggests that cutoff variation does not represent a reliable approach to uncertainty quantification, which is fully in line with the conclusions of [35]. Regulator artifacts in uniform matter have also been addressed in Ref. [61].

In this letter we calculate, for the first time, the properties of symmetric nuclear matter (SNM) and pure neutron matter (PNM) based the latest generation of chiral NN potentials up to $N^4\text{LO}$ of Refs. [35, 36] using the BHF theory. The purpose of our study is twofold. First, we explore the suitability of the most recent generation of the chiral forces for microscopic description of the equation of state (EOS) of SNM and PNM. Second, by performing an error analysis along the lines of Refs. [35, 36, 41] without relying on cutoff variation, we estimate the theoretical accuracy in the description of the nuclear EOS achievable at various orders of the chiral expansion. Our paper is organized as follows. In section 2 we briefly outline our calculation approach based on the BHF theory. The results of our calculations are presented in section 3

for all available cutoff values, while the theoretical uncertainty from the truncation of the chiral expansion is quantified in section 4. Finally, the main conclusions of our paper are summarized in section 5.

2. Brueckner-Hartree-Fock theory

In the BHF theory of nuclear matter, the underlying NN potential, determined by the NN scattering data, is replaced by an effective NN interaction, i.e. the G -matrix, which can be calculated by solving the Bethe-Goldstone equation [57, 62],

$$G[\omega, \rho] = V + \sum_{k_a, k_b > k_F} V \frac{|k_a k_b\rangle \langle k_a k_b|}{\omega - e(k_a) - e(k_b) + i\epsilon} G[\omega, \rho], \quad (1)$$

where V is the underlying NN potential provided by chiral EFT, ρ is the nucleon number density, and ω the starting energy. The single-particle energy is

$$e(k) = e(k; \rho) = \frac{k^2}{2m} + U(k, \rho). \quad (2)$$

The continuous choice for the single-particle potential $U(k, \rho)$ used in the present BHF theory [62] has the form

$$U(k; \rho) = \text{Re} \sum_{k' < k_F} \langle kk' | G[e(k) + e(k'); \rho] | kk' \rangle_a, \quad (3)$$

where the subscript a indicates antisymmetrization of the matrix elements. These coupled equations are solved in a self-consistent way. Finally, in the BHF theory, we obtain the energy per nucleon as

$$\frac{E}{A} = \frac{3}{5} \frac{k_F^2}{2m} + \frac{1}{2\rho} \text{Re} \sum_{k, k' < k_F} \langle kk' | G[e(k) + e(k'); \rho] | kk' \rangle_a. \quad (4)$$

3. Results

In Fig. 1, we show our results for the density dependence of the energy per nucleon of symmetric nuclear matter and pure neutron matter for all available chiral orders and cutoff values, where the G -matrices are solved up to the partial waves $J = 6$. We remind the reader that the long-range contributions are regularized in the newest chiral NN potentials by multiplying the corresponding coordinate-space expressions with the function

$$f(r) = \left[1 - \exp\left(-\frac{r^2}{R^2}\right) \right]^n, \quad n = 6, \quad R = 0.8 \dots 1.2 \text{ fm}. \quad (5)$$

For contact interactions, a non-local Gaussian regulator in momentum space is employed with the cutoff Λ being related to R via $\Lambda = 2/R$. We emphasize that the calculations reported in this paper do not include the contributions of three- and four-nucleon forces and are thus incomplete starting from N²LO.

For SNM, the LO (i.e. Q^0), NLO (i.e. Q^2) and N⁴LO NN potentials yield larger binding energies for softer interactions (i.e. for larger cutoffs R), while the situation is opposite at N²LO and N³LO. For PNM, the harder (softer) interactions yield more (less) attraction at LO...N³LO (N⁴LO). This complicated pattern suggests that the EOS is rather sensitive to the details of the nuclear force and especially to the interplay between its intermediate and short-range components which is expected to be strongly regulator dependent. Our results at NLO agree well with the ones reported in [59] both for SNM and PNM² and with the Quantum Monte Carlos calculation of [38] for PNM. Interestingly, the cutoff dependence of the energy per particle of

²We cannot compare our N²LO and N³LO predictions with those of [59] since no results based on NN interactions only are provided in that work.

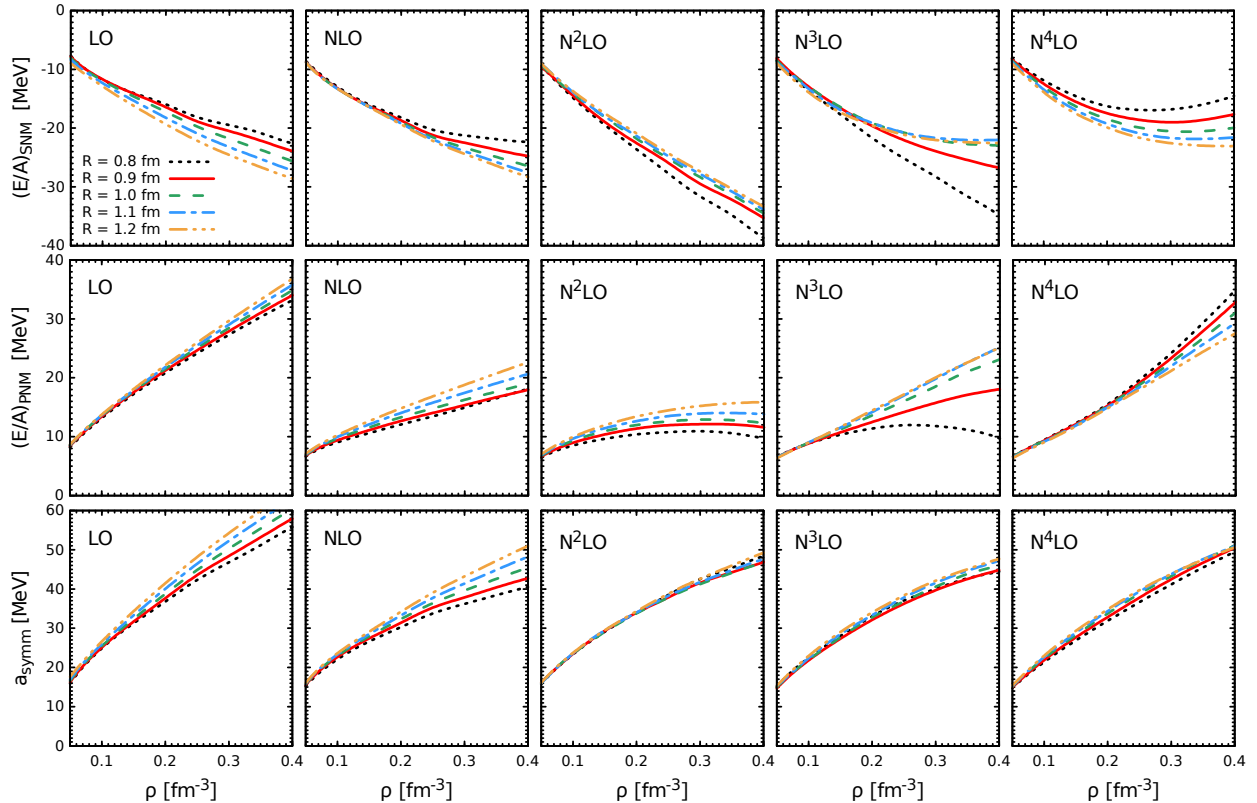


Figure 1: (Color online) Density dependence of the energy per particle of SNM $(E/A)_{\text{SNM}}$ (upper row), PNM $(E/A)_{\text{PNM}}$ (middle row) and of the symmetry energy a_{symm} (lower row) based on chiral NN potentials of [35, 36] for all available cutoff values in the range of $R = 0.8 \dots 1.2$ fm.

Table 1: Saturation properties of SNM based on the AV18 potential and the $N^4\text{LO}$ chiral NN potentials for all available cutoff values.

	AV18	$N^4\text{LO}_{R=0.8\text{ fm}}$	$N^4\text{LO}_{R=0.9\text{ fm}}$	$N^4\text{LO}_{R=1.0\text{ fm}}$	$N^4\text{LO}_{R=1.1\text{ fm}}$	$N^4\text{LO}_{R=1.2\text{ fm}}$
ρ_{sat} (fm^{-3})	0.26	0.28	0.29	0.31	0.35	0.40
E/A (MeV)	-17.78	-17.14	-19.15	-20.67	-21.92	-23.28
M^*/M	0.71	0.74	0.73	0.72	0.72	0.71

PNM at NLO is qualitatively different from the one found in [59] which demonstrates that the form of the regulator does significantly affect the properties of the resulting potentials.

Generally, our results for both SNM and PNM show an increasing attraction in the NN force when going from LO to $N^2\text{LO}$, that can probably be traced back to the two-pion exchange potential (TPEP), which has a very strong attractive central isoscalar piece. At $N^3\text{LO}$, the chiral TPEP receives further attractive contributions but also develops a repulsive short-range core. The additional repulsion at $N^4\text{LO}$ comes from the contributions to the TPEP at this order. The EOSs based on the $N^3\text{LO}$ and $N^4\text{LO}$ potentials alone show saturation points below $\rho = 0.4 \text{ fm}^{-3}$ except for $N^3\text{LO}$ at $R = 0.8$ fm and $R = 0.9$ fm.

It is instructive to compare the results based on the most accurate chiral potentials at $N^4\text{LO}$ with the ones from high-precision phenomenological interactions such as the AV18 potential [9]. In Table. 1, we list the saturation properties, saturation densities and saturation binding energies per particle, and the effective

Table 2: Contributions of the various partial waves (in units of MeV) to the binding energies of SNM at the corresponding saturation densities for the AV18 and chiral N⁴LO NN potentials for all available cutoff values.

	AV18	N ⁴ LO _{R=0.8 fm}	N ⁴ LO _{R=0.9 fm}	N ⁴ LO _{R=1.0 fm}	N ⁴ LO _{R=1.1 fm}	N ⁴ LO _{R=1.2 fm}
¹ S ₀	-20.71	-18.97	-20.22	-21.41	-23.03	-24.68
³ P ₀	-4.74	-4.92	-5.06	-5.31	-5.75	-6.21
³ S ₁ - ³ D ₁	-21.91	-23.83	-24.87	-25.80	-26.60	-27.27
³ P ₁	16.68	18.29	19.07	20.62	23.78	27.64
¹ P ₁	6.22	7.02	7.23	7.75	8.83	10.16
³ P ₂ - ³ F ₂	-13.96	-15.92	-16.68	-18.17	-21.23	-25.25
¹ D ₂	-4.94	-5.44	-5.71	-6.29	-7.49	-9.05
³ D ₂	-6.89	-7.62	-7.97	-8.66	-10.05	-11.78
³ D ₃ - ³ G ₃	0.25	0.49	0.46	0.43	0.39	0.28
¹ F ₃	1.44	1.55	1.62	1.76	2.03	2.37
³ F ₃	2.65	2.93	3.06	3.35	3.90	4.58
³ F ₄ - ³ H ₄	-1.02	-1.26	-1.32	-1.46	-1.76	-2.12
¹ G ₄	-0.88	-1.00	-1.06	-1.17	-1.41	-1.72
³ G ₄	-1.47	-1.65	-1.74	-1.93	-2.34	-2.87

Table 3: Contributions of the various partial waves (in units of MeV) to the binding energies of SNM at the empirical saturation density, $\rho = 0.16 \text{ fm}^{-3}$, for the AV18 and chiral N⁴LO NN potentials for all available cutoff values.

	AV18	N ⁴ LO _{R=0.8 fm}	N ⁴ LO _{R=0.9 fm}	N ⁴ LO _{R=1.0 fm}	N ⁴ LO _{R=1.1 fm}	N ⁴ LO _{R=1.2 fm}
¹ S ₀	-15.01	-14.32	-14.83	-15.19	-15.47	-15.81
³ P ₀	-3.07	-3.17	-3.17	-3.18	-3.18	-3.18
³ S ₁ - ³ D ₁	-18.74	-19.72	-20.18	-20.68	-20.78	-20.93
³ P ₁	8.47	9.16	9.17	9.14	9.15	9.14
¹ P ₁	3.36	3.61	3.59	3.57	3.56	3.55
³ P ₂ - ³ F ₂	-6.89	-7.71	-7.71	-7.73	-7.74	-7.79
¹ D ₂	-2.26	-2.45	-2.45	-2.47	-2.50	-2.55
³ D ₂	-3.34	-3.65	-3.65	-3.66	-3.67	-3.68
³ D ₃ - ³ G ₃	0.08	0.20	0.19	0.16	0.13	0.09
¹ F ₃	0.66	0.72	0.72	0.72	0.72	0.72
³ F ₃	1.19	1.31	1.30	1.30	1.30	1.29
³ F ₄ - ³ H ₄	-0.34	-0.41	-0.41	-0.40	-0.39	-0.38
¹ G ₄	-0.35	-0.39	-0.39	-0.39	-0.39	-0.39
³ G ₄	-0.57	-0.64	-0.64	-0.63	-0.63	-0.63

mass of the nucleon [60]:

$$\frac{M^*}{M} = 1 - \frac{dU(k; e(k))}{de(k)}, \quad (6)$$

at the saturation point for the AV18 and N⁴LO potentials, while the contributions of the various partial waves up to $J = 4$ to the potential energy per nucleon at the saturation density are given in Table 2. Notice that the listed saturation properties are still far from the empirical data ($\rho_{\text{sat}} \sim 0.16 \text{ fm}^{-3}$ and $E/A \sim 16 \text{ MeV}$) due to the missing 3NF contributions [57, 62]. Naturally, we observe that the results based on the hardest version of the N⁴LO potential with $R = 0.8 \text{ fm}$ are rather similar to those based on AV18. Interestingly, we find that the partial wave contributions to the energy increase when the N⁴LO potentials

are softened by increasing the coordinate-space cutoff R (except for the 3D_3 - 3G_3 channel). In Table 3, the partial wave contributions to potential energy at the empirical saturation density, $\rho = 0.16 \text{ fm}^{-3}$ for different NN potentials are listed from 1S_0 to 3G_4 states. It is found that all contributions are nearly cutoff-independent except the ones from 1S_0 , 3S_1 - 3D_1 , and 3D_3 - 3G_3 states, which are decreasing with the cutoffs R . Actually, the size of these contributions is strongly dependent on the central and tensor components in the NN potential. The larger cutoff R corresponds to stronger short-range correlations and removes more repulsive contribution on the NN potential at short distance. It will generate more attractive binding energy. Our results for the saturation density and binding energy confirm the linear correlation between these two quantities known as the Coester line [63], see also [57]. Calculations within the BHF theory using phenomenological potentials have revealed that the position on the Coester line is correlated with the deuteron D -state probability P_D with smaller values of P_D typically resulting in smaller saturation energy and density [6, 57]. We do not observe this correlation for the chiral N⁴LO potentials with $P_D = 4.28\%$ ($P_D = 5.12\%$) for $R = 0.8 \text{ fm}$ ($R = 1.2 \text{ fm}$). This is similar to the lack of correlation between P_D and the triton binding energy for the novel chiral potentials [41]. We remind the reader that the D -state probability is not an observable.

We have also extracted the symmetry energy of nuclear matter $a_{\text{symm}}(\rho)$, the quantity which describes the response of the nuclear force on excess neutrons or protons and plays an important role in understanding the properties of nuclei and astrophysical objects. The symmetry energy $a_{\text{symm}}(\rho)$ is defined in terms of the expansion of the asymmetric nuclear matter in powers of the asymmetry parameter $\delta \equiv (\rho_n - \rho_p)/\rho$, with ρ_n and ρ_p referring to the neutron and proton number densities, via

$$\frac{E}{A}(\rho, \delta) = \frac{E}{A}(\rho, 0) + a_{\text{symm}}(\rho) \delta^2 + \dots \quad (7)$$

The terms beyond the quadratic one are known to be very small [64], so that the symmetry energy can be well approximated by

$$a_{\text{symm}}(\rho) = \left(\frac{E}{A} \right)_{\text{PNM}} - \left(\frac{E}{A} \right)_{\text{SNM}}, \quad (8)$$

where E/A is viewed as a function of ρ and δ . While the calculated symmetry energies show significant cutoff dependence at LO and NLO, which is comparable to that of $(E/A)_{\text{SNM}}$ and $(E/A)_{\text{PNM}}$, the results at higher orders are almost insensitive to the values of R and show a little variation with the order of the chiral expansion. The resulting value of $a_{\text{symm}} = 27.9 - 30.5 \text{ MeV}$ at the empirical saturation density, calculated using the N⁴LO potentials, is consistent with the empirical constraints and the results from the phenomenological high-precision NN potentials [57] with $a_{\text{symm}} = 28.5 - 32.6 \text{ MeV}$ at $\rho = 0.17 \text{ fm}^{-3}$ and the ones from the functional renormalization group method with $a_{\text{symm}} = 29.0 - 33.0 \text{ MeV}$ at $\rho = 0.16 \text{ fm}^{-3}$ [55]. Furthermore, Vidaña *et al.* also studied the properties of the symmetry energy with AV 18 potential plus a phenomenological three-body force as Urbana type [66]. However, it is found that the isovector properties of nuclear matter are not affected by the three-body force too much.

4. Uncertainty quantification

We now turn to the important question of uncertainty quantification from the truncation of the chiral expansion. Actually, Baldo *et al.* attempted to quantify the theoretical uncertainties of the EOSs with the family of Argonne NN potential through comparing the BHF theory to other many-body approaches [65]. These uncertainties are strongly dependent on the methodologies of nuclear many-body approximation to treat the spin structures of potentials. Here we follow the approach formulated in Ref. [35], which makes use of the explicitly known contributions to an observable of interest at various chiral orders to estimate the size of truncated terms *without relying on cutoff variation*. The algorithm proposed in [35] has been adjusted in Ref. [41] to enable applications to incomplete few- and many-nucleon calculations based on two-nucleon forces only. Here and in what follows, we use the method as formulated in that paper, which was also employed in [42]. Specifically, for an observable $X(p)$ with p referring to the corresponding center-of-mass

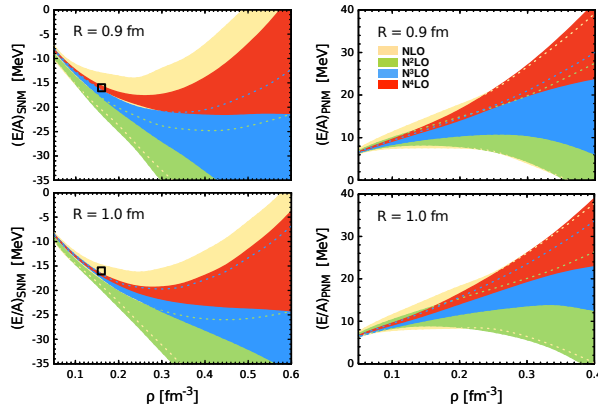


Figure 2: (Color online) Predictions for the EOS of SNM (left panel) and PNM (right panel) based on the chiral NN potentials of Refs. [35, 36] for $R = 0.9$ fm (upper row) and $R = 1.0$ fm (lower row) along with the estimated theoretical uncertainties. Open rectangles visualize the empirical saturation point of symmetric nuclear matter.

momentum scale, the theoretical uncertainty $\delta X^{(i)}$ of the i -th chiral order prediction $X^{(i)}$ is estimated via

$$\begin{aligned}
 \delta X^{(0)} &= \max(Q^2 |X^{(0)}|, |X^{(\geq 0)} - X^{(\geq 0)}|), \\
 \delta X^{(2)} &= \max(Q^3 |X^{(0)}|, Q |\Delta X^{(2)}|, Q \delta X^{(0)}, |X^{(\geq 2)} - X^{(\geq 2)}|), \\
 \delta X^{(i)} &= \max(Q^{i+1} |X^{(0)}|, Q^{i-1} |\Delta X^{(2)}|, Q^{i-2} |\Delta X^{(3)}|, Q \delta X^{(i-1)}) \quad \text{for } i \geq 3,
 \end{aligned} \tag{9}$$

where $Q = \max(p/\Lambda_b, M_\pi/\Lambda_b)$ is the estimated expansion parameter while $\Delta X^{(2)} \equiv X^{(2)} - X^{(0)}$ and $\Delta X^{(i)} \equiv X^{(i)} - X^{(i-1)}$, $i > 2$, denote the chiral-order Q^2 and Q^i contributions to $X(p)$. The breakdown scale of the nuclear chiral EFT was estimated to be $\Lambda_b \simeq 600$ MeV [35].³ The Bayesian analysis of the chiral EFT predictions for the NN total cross section of Ref. [67] has revealed, that the actual breakdown scale may even be a little higher than $\Lambda_b \simeq 600$ MeV for $R = 0.9$ fm.

In Fig. 2, we show the results for the EOS for SNM and PNM including the estimated theoretical uncertainties at various orders of the chiral expansion for the most accurate versions of the NN potentials with $R = 0.9$ fm and $R = 1.0$ fm [35, 36]. The expansion parameter Q at a given density is estimated by identifying the momentum scale p with the Fermi momentum k_F , which is related to the density ρ via $\rho = 2k_F^3/(3\pi^2)$ ($\rho = k_F^3/(3\pi^2)$) for SNM (PNM), and assuming $\Lambda_b = 600$ MeV. At the saturation density, the achievable accuracy of the chiral EFT predictions for the energy per particle may be expected to be about ± 1.5 MeV (± 0.3 MeV) for SNM and ± 2 MeV (± 0.7 MeV) for PNM at N²LO (N⁴LO). Notice that the expected accuracy at N⁴LO is significantly smaller than the current model dependence for these quantities. We further emphasize that the presented estimations should be taken with some care due to the non-availability of complete calculations beyond NLO. More reliable estimations of the theoretical uncertainty using the approach of [35] will be possible once the corresponding three- and four-nucleon forces are included.

Our results confirm the conclusions of [59] that cutoff variation does not provide an adequate way for estimating the uncertainties in the calculations of the nuclear EOS. As discussed in [35], the residual cutoff-dependence of observables may generally be expected to underestimate the theoretical uncertainty at NLO and N³LO, which is consistent with our results. Further, the spread of results for different values of R at N⁴LO appears to be roughly of a similar size as the estimated uncertainty at this order. We, however, refrain from drawing more definite conclusions on the cutoff dependence based on the incomplete calculations.

Finally, we have also quantified the achievable accuracy of the theoretical determination of the symmetry energy a_{symm} and the slope parameter L , defined as $L = 3\rho \partial(E/A)_{\text{SNM}}/\partial\rho$, at the empirical saturation density. These important quantities have been constrained by the available experimental information on

³To account for increasing finite-cutoff artefacts using softer versions of the chiral forces, the lower values of $\Lambda_b = 500$ MeV and 400 MeV were employed in calculations based on $R = 1.1$ fm and $R = 1.2$ fm, respectively.

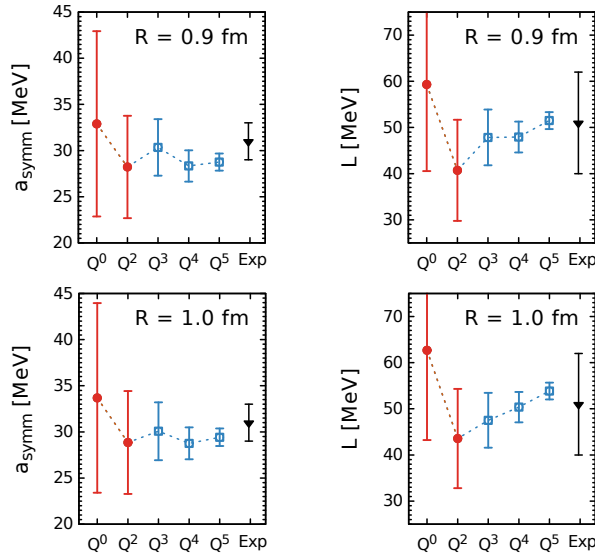


Figure 3: (Color online) Chiral expansion of the symmetry energy a_{symm} (left panel) and the slope parameter L (right panel) at the empirical saturation density of $\rho = 0.16 \text{ fm}^{-3}$ for the cutoff values of $R = 0.9$ fm (upper row) and $R = 1.0$ fm (lower row) along with the estimated theoretical uncertainty. Solid circles (open rectangles) show the complete results at a given chiral order (incomplete results based on NN interactions only). Solid triangles show the current experimental constraints on a_{symm} and L as described in the text.

e.g. neutron skin thickness, heavy ion collisions and dipole polarizabilities leading to the ranges of $29 \text{ MeV} \lesssim a_{\text{symm}} \lesssim 33 \text{ MeV}$ and $40 \text{ MeV} \lesssim L \lesssim 62 \text{ MeV}$ [68, 69, 70]. In Fig. 3, we show our results for these quantities using the NN potentials from LO to $N^4\text{LO}$ along with the estimated theoretical uncertainties. Especially for the slope parameter, a complete calculation at $N^4\text{LO}$ would yield a theoretical prediction much more accurate than the current experimental data.

5. Summary and conclusions

In summary, we calculated the equations of state (EOSs) of SNM and PNM with the state-of-the-art chiral NN potentials from LO to $N^4\text{LO}$ in the framework of Brueckner-Hartree-Fock theory. At $N^4\text{LO}$, the EOS of SNM has saturation points for all employed cutoff values with the corresponding saturation densities and binding energies per particle being within the range of $0.28 \dots 0.40 \text{ fm}^{-3}$ and $-17.14 \dots -23.28 \text{ MeV}$, respectively. These values are compatible with the ones based on the phenomenological high-precision potentials like e.g. the AV18 potential. The symmetry energy and the slope parameter at the saturation density are found to be in the range of $a_{\text{symm}} = 27.9 \dots 30.5 \text{ MeV}$ and $L = 49.4 \dots 55.0 \text{ MeV}$, respectively, using the $N^4\text{LO}$ potentials with the cutoff in the range of $R = 0.8 \dots 1.2 \text{ fm}$.

We have also estimated the achievable theoretical accuracy at various orders in the chiral expansion using the novel approach formulated in Refs. [35, 41] and discussed the convergence of the chiral expansion. Similar to [59], we find that the residual cutoff dependence of the energy per particle does not allow for a reliable estimation of the theoretical uncertainty, see also the discussion in Ref. [35]. We find that chiral EFT may be expected to provide an accurate description of SNM and PNM at the saturation density, with the expected accuracy of a few percent at $N^4\text{LO}$. At this order, a semi-quantitative description of the EOS should be possible up to about twice the saturation density of nuclear matter. Clearly, this will require a consistent inclusion of the corresponding many-body forces. Work along these lines is in progress to compare with the existing calculations with two-body and three-body chiral force [52, 59].

Acknowledgments

We would like to thank Arnau Rios Huguet for sharing his insights into the topics discussed here. UGM thanks the ITP (CAS, Beijing) for hospitality, where part of this work was done. This work was supported in part by the National Natural Science Foundation of China (Grant Nos. 11335002, 11405090, 11405116 and 11621131001), DFG (SFB/TR 110, “Symmetries and the Emergence of Structure in QCD”) and BMBF (contract No. 05P2015 -NUSTAR R&D). The work of UGM was supported in part by The Chinese Academy of Sciences (CAS) President’s International Fellowship Initiative (PIFI) grant no. 2015VMA076.

References

- [1] H. Yukawa, Proc. Phys. Math. Soc. Japan 17 (1935) 48.
- [2] M. Taketani, S. Nakamura, M. Sasaki, Prog. Theor. Phys. 6 (1951) 581.
- [3] P. Signell, Adv. Nucl. Phys. 2 (1969) 223.
- [4] K. Erkelenz, Phys. Rep. 13 (1974) 191.
- [5] R. Machleidt, K. Holinde, Ch. Elster, Phys. Rep. 149 (1987) 1.
- [6] R. Machleidt, Adv. Nucl. Phys. 19 (1989) 189.
- [7] V. G. J. Stoks, R. A. M. Klomp, C. P. F. Terheggen, J. J. de Swart, Phys. Rev. C 49 (1994) 2950.
- [8] R. B. Wiringa, R. A. Smith, T. L. Ainsworth, Phys. Rev. C 29 (1984) 1207.
- [9] R. B. Wiringa, V. G. J. Stoks, R. Schiarilla, Phys. Rev. C 51 (1995) 38.
- [10] R. Machleidt, Phys. Rev. C 63 (2001) 024001.
- [11] S. Weinberg, Phys. Lett. B 251 (1990) 288.
- [12] S. Weinberg, Nuclear Phys. B 363 (1991) 3.
- [13] S. Weinberg, Phys. Lett. B 295 (1992) 114.
- [14] C. Ordóñez, L. Ray, U. van Kolck, Phys. Rev. Lett. 72 (1994) 1982.
- [15] C. Ordóñez, L. Ray, U. van Kolck, Phys. Rev. C 53 (1996) 2086.
- [16] E. Epelbaum, W. Glöckle, U.-G. Meißner, Nucl. Phys. A 637 (1998) 107.
- [17] E. Epelbaum, W. Glöckle, U.-G. Meißner, Nucl. Phys. A 671 (2000) 295.
- [18] E. Epelbaum, W. Glöckle, U.-G. Meißner, Nucl. Phys. A 747 (2005) 362.
- [19] D. R. Entem, R. Machleidt, Phys. Rev. C 68 (2003) 041001.
- [20] N. Kaiser, Phys. Rev. C 62 (2000) 024001.
- [21] N. Kaiser, Phys. Rev. C 61 (2000) 014003.
- [22] N. Kaiser, Phys. Rev. C 64 (2001) 057001.
- [23] S. Ishikawa, M. R. Robilotta, Phys. Rev. C 76 (2007) 014006.
- [24] V. Bernard, E. Epelbaum, H. Krebs, U.-G. Meißner, Phys. Rev. C 77 (2008) 064004.
- [25] V. Bernard, E. Epelbaum, H. Krebs, U.-G. Meißner, Phys. Rev. C 84 (2011) 054001.
- [26] E. Epelbaum, Phys. Lett. B 639 (2006) 456.
- [27] E. Epelbaum, Eur. Phys. J. A 34 (2007) 197.
- [28] E. Epelbaum, H. W. Hammer, U.-G. Meißner, Rev. Mod. Phys. 81 (2009) 1773.
- [29] R. Machleidt, D. R. Entem, Phys. Rep. 503 (2011) 1.
- [30] H. Krebs, A. Gasparyan, E. Epelbaum, Phys. Rev. C 85 (2012) 054006.
- [31] H. Krebs, A. Gasparyan, E. Epelbaum, Phys. Rev. C 87 (2013) 054007.
- [32] L. Girlanda, A. Kievsky, M. Viviani, Phys. Rev. C 84 (2011) 014001.
- [33] D. R. Entem, N. Kaiser, R. Machleidt, Y. Nosyk, Phys. Rev. C 91 (2015) 014002.
- [34] D. R. Entem, N. Kaiser, R. Machleidt, Y. Nosyk, Phys. Rev. C 92 (2015) 064001.
- [35] E. Epelbaum, H. Krebs, U.-G. Meißner, Eur. Phys. J. A 51 (2015) 53.
- [36] E. Epelbaum, H. Krebs, U.-G. Meißner, Phys. Rev. Lett. 115 (2015) 122301.
- [37] V. G. J. Stoks, R. A. M. Klomp, M. C. M. Rentmeester, J. J. de Swart, Phys. Rev. C 48 (1993) 792.
- [38] A. Gezerlis *et al.*, Phys. Rev. Lett. 111 (2013) 032501.
- [39] M. Piarulli *et al.*, Phys. Rev. C 91 (2015) 024003.
- [40] see <http://www.lenpic.org>.
- [41] S. Binder, *et al.* (LENPIC Collaboration), Phys. Rev. C 93 (2016) 044002.
- [42] R. Skibinski *et al.*, Phys. Rev. C 93 (2016) 064002.
- [43] J. Carlson *et al.*, Rev. Mod. Phys. 87 (2015) 1067.
- [44] W. H. Dickhoff and C. Barbieri, Prog. Part. Nucl. Phys. 52 (2004) 377.
- [45] G. Hagen, T. Papenbrock, M. Hjorth-Jensen, and D. J. Dean, Rep. Prog. Phys. 77 (2014) 096302.
- [46] D. Lee, Prog. Part. Nucl. Phys. 63 (2009) 117.
- [47] E. Epelbaum *et al.*, Phys. Rev. Lett. 112 (2014) 102501.
- [48] U.-G. Meißner, Nucl. Phys. News. 24 (2014) no.4, 11.
- [49] B. R. Barrett, P. Navratil, and J. P. Vary, Prog. Part. Nucl. Phys. 69 (2013) 131.
- [50] S. H. Shen *et al.*, Chin. Phys. Lett. 33 (2016) 102103.
- [51] A. Carbone, A. Polls, A. Rios, Phys. Rev. C 88 (2013) 044302.
- [52] A. Carbone, A. Rios, A. Polls, Phys. Rev. C 90 (2014) 054322.

- [53] G. Hagen *et al.*, Phys. Rev. C 89 (2014) 014319.
- [54] C. Drischler, V. Somà, A. Schwenk, Phys. Rev. C 89 (2014) 025806.
- [55] M. Drews, W. Weise, Phys. Rev. C 91 (2015) 035802.
- [56] M. Drews, W. Weise, Prog. Part. Nucl. Phys. in press, (2016).
- [57] Z. H. Li *et al.*, Phys. Rev. C 74 (2006) 047304.
- [58] R. Machleidt, P. Liu, D. R. Entem, E. Ruiz Arriola, Phys. Rev. C 81 (2010) 024001.
- [59] F. Sammarruca *et al.*, Phys. Rev. C 91 (2015) 054311.
- [60] A. Li, J. N. Hu, X. L. Shang, W. Zuo, Phys. Rev. C 93 (2016) 015803.
- [61] A. Dyhdalo, R. J. Furnstahl, K. Hebeler, I. Tews, Phys. Rev. C 94 (2016) 034001.
- [62] M. Baldo, C. Maieron, J. Phys. G 34 (2007) R243.
- [63] F. Coester, S. Cohen, B. Day, C. M. Vincent, Phys. Rev. C 1 (1970) 769.
- [64] C. Drischler, K. Hebeler, A. Schwenk, Phys. Rev. C 93 (2016) 054314 .
- [65] M. Baldo, A. Polls, A. Rios, H.-J. Schulze, I. Vidaña, Phys. Rev. C 86 (2012) 064001.
- [66] I. Vidaña, C. Providência, A. Polls, A. Rios, Phys. Rev. C 80 (2009) 045806.
- [67] R. J. Furnstahl, N. Klco, D. R. Phillips, S. Wesolowski, Phys. Rev. C 92 (2015) 024005.
- [68] M. B. Tsang *et al.*, Phys. Rev. C 86 (2012) 015803.
- [69] J. M. Lattimer, Y. Lim, Astrophys. J. 771 (2013) 51 .
- [70] J. M. Lattimer, A. W. Steiner, Eur. Phys. J. A 50 (2014) 40.